2023 IEEE/ASME International Conference on Advanced Intelligent Mechatronics (AIM)
June 28-30, 2023. Seattle, Washington, USA

Design and Prototyping of a Miniature Gripper with Decoupled Wrist and Rolling Capabilities for Robotic Surgery

Mohamed Sallam[1,2], Giuseppe Andrea Fontanelli[1] and Fanny Ficuciello[1]

***Abstract*— This paper proposes a design of a miniature gripper that can drive a suture needle in Robot-assisted Surgery. The presented gripper has two more advantages over the standard needle driver of da Vinci surgical robot. Firstly, it has a decoupled wrist that allows all joints to rotate independently of each other with no coupling between them. This in turn lets the control strategy to be less complicated since each DOF is actuated by only one motor. Secondly, it has rolling capabilities, similar to the human hand, that allow re-orienting the needle with only two fingers. The gripper is rapid prototyped and tested using a drive unit that is designed and developed in this work specifically for this purpose. Two experiments are conducted to validate the proposed design; in the first experiment the gripper is actuated about the wrist axis while the end effector position is measured and compared with the expected trajectory. The results showed that the wrist is completely decoupled from the other joints, as only a slight variation of 1% was obtained. In the second experiment, the motion capabilities of the gripper are demonstrated, and the rolling functionality is tested in presence of a surgical needle.**

I. INTRODUCTION

Robotic-assisted surgery offers many benefits to physicians and patients compared to open or traditional minimally invasive surgery (MIS). It allows surgeons to conduct operations in hard-to-reach areas through tiny incisions with precise movements and enhanced vision. It also improves surgeons decision making during operation by providing them with information about the interaction with the organs they are operating on [1], [2]. The benefits for patients include less blood loss, less post-operative pain, less risk of infection and less recovery time. Motivated by these advantages, robot-assisted MIS has been widely adopted by many hospitals and medical centers all over the world. The company of Intuitive Surgical, the manufacturer of da Vinci surgical robots, disclosed in its annual report [3] that worldwide da Vinci procedures in 2021 grew approximately 28% compared with 2020, and the increase in shipping new da Vinci systems during the same period was up to 44%.

To expand the range of procedures that robots can perform, the surgical tools have to be continuously improved to enhance the robot's dexterity and functionality [5], [6]. The standard tool, currently used by da Vinci robot, has an articulated gripper known as EndoWrist with four controllable DOFs. It allows surgeons to grasp objects and perform rotations about the roll, wrist and yaw axes inside the human body, Fig. 1. The gripper is mounted on one end of the tool, and actuated by a drive unit placed on the other end, outside the human body, while the motion and forces are transmitted by cables. By design, the joints at the wrist and yaw axes are coupled together. This means, when the wrist is actuated, the joints on the yaw axis will rotate as well. Such a rotation about the yaw axis is undesirable if only a pure rotation about the wrist is desired. This problem is solved electronically by coordinating the control of the actuators to compensate for the undesired motion. However, it is preferred to have a gripper with mechanically decoupled joints than having a gripper with coupled but electronically coordinated joints for three reasons. Firstly, the gripper with decoupled wrist requires less complicated control scheme as each joint is actuated independently by only one motor [7]. Secondly, from safety point of view during surgical operations, it has been reported that decoupled mechanisms are preferred to be used in tools and instruments [8]. Thirdly, the interaction forces between the gripper and environment can be directly estimated by measuring the tension in the drive cables using sensors placed outside the human body [9], [10]. This in turn helps to avoid the practical problems of using direct force sensors mounted on the very small surface of the graspers inside the human body [11].

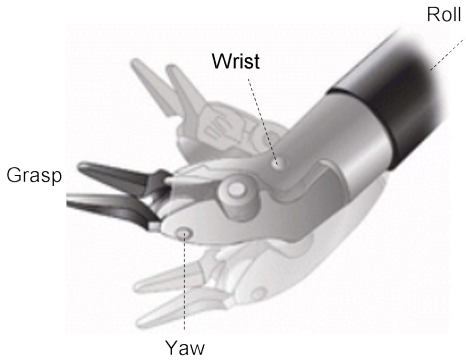

Fig. 1: Standard EndoWrist of da Vinci Surgical System [4]

In the literature, several mechanically decoupled grippers have been presented to be used in robotic-assisted MIS. Grace in [12] proposed a design of a gripper with decoupled wrist that allows grasping, suturing and cutting in the human tissue. However, the operating range of the gripper jaw was quite limited as only one of the two graspers was allowed to rotate while the other one was fixed. In addition, the motion and forces were transferred from the actuators to the gripper using rigid-link mechanisms which reduces the

[1]The authors are with the ICAROS Lab, Department of Electrical Engineering and Information Technology, University of Naples Federico II, Naples, 80131, Italy. Corresponding author's e-mail: mohamedabdelghany.sallam@unina.it

[2]Mohamed Sallam is also with the Department of Mechanical Engineering, Helwan University, Cairo, Egypt.

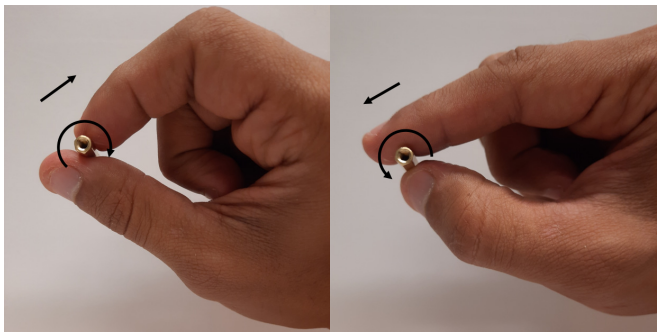

Fig. 2: Human hand rolling capabilities

device reliability due to the wearing, friction and clearance between the mechanical parts. More advanced decoupled mechanisms, that can operate in larger workspace, were presented by Zhao and Nelson in [7], Nishizawa and Kishi in [13] and Kwon et al. in [14]. However, the complexity of the design that has several gears and pulleys affected the device safety, efficiency and reliability during operation.

A new concept of decoupled grippers was presented in [15] by Moreyra and in [16] by Tadano and Kawashima. In their approach, they routed the tendons through the symmetry plane of the tool wrist. The tendons extended from the centre of the wrist to the graspers mounted on yaw axis across non-movable pulleys. The grippers were compact and with a fewer mechanical parts. However, the pulleys on yaw axis were not positioned in such a way that the centre lines of the tendons are aligned with the mid-planes of the pulleys as defined by the law of belting in [17]. That may cause the rope to slip out of the pulley groove leading to drive failure. Moreover, the rope may suffer fraying if it is rubbing strongly against the pulley edge. Brock and Lee in [18] proposed a gripper that exploits the concept of guiding the tendons through the symmetry plane of the wrist but using two fixed pairs of tubes instead of the non-movable pulleys to avoid the slipping of the tendons out of the grooves. However, the joints suffered some coupled effect due to the stretching of the tendons in some configurations when the tool is actuated about the wrist axis. Mei et al. in [19] and Niu et al. in [20] presented a new design of a surgical gripper that has a coupled wrist integrated with a set of gears that can mechanically compensate the undesired motion. The gears could completely eliminate the coupling between the joints but with two concerns. The first is about the problems associated with using multiple gears in medical application that is very sensitive to any backlash or clearance between the mechanical parts. The second concern was that the design did not follow the law of belting. Other ideas and improvements of surgical tools with decoupled wrist are presented in [21], [22], [23], [24], [25] and [26].

On the other side, one of the missing functionalities in surgical grippers is the ability to roll an object in a similar manner to the human hand (see Fig. 2). Such a rolling capability is quite helpful during tissue suturing and reconstructive procedures where surgeons may need to change

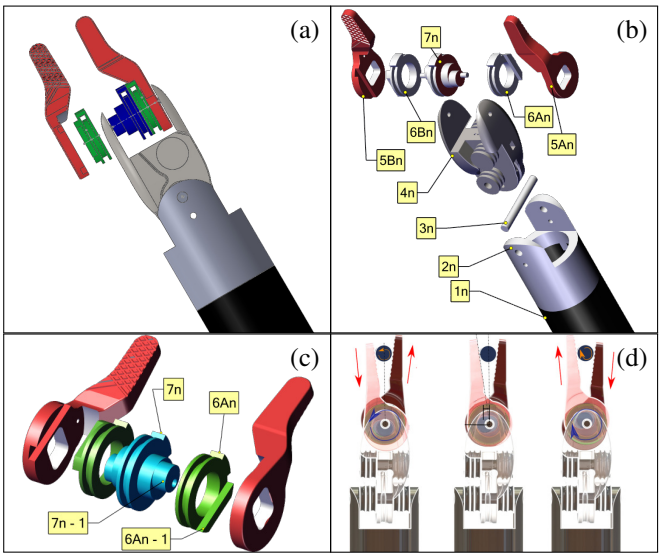

Fig. 3: Tool prior design with coupled wrist and rolling capabilities [28].

frequently the needle orientation to reach an appropriate pose. A new concept of needle driver with rolling capabilities was presented for the first time in our previous work [28]. The tool allowed surgeons to change the needle orientation with only one arm. The only concern was the mechanical coupling between the wrist and yaw joints which complicates the control strategy.

In this research, we propose a modified design of our tool, that has been presented previously in [28], to have a decoupled wrist along with its rolling capabilities. The proposed design is based on the approach of routing the tendons through the symmetry plane of the gripper wrist across fixed posts. Firstly, we analyse the joint coupling in the prior design, and derive a transmission matrix that describes the relation between the actuators and the driven pulleys. Afterwards, we present the prototype of the new design that has been realized using a metal 3D printer to validate the decoupling mechanism, and evaluate its motion capabilities. In addition, an actuation unit with 5 actuators is developed in this work to drive-by-wire the five degrees of freedom of the tool. Two experiments are conducted to test the gripper and demonstrate its functionalities.

The remainder of this article is organized as follows. Section II describes the prior design and the joint coupling of the tool. Section III presents the design of the new gripper with decoupled mechanism. Section IV presents the design of the actuation unit. Section V presents the kinematic model of the new tool. Section VI presents the prototype, experiments and obtained results. Finally, section VII concludes this article and provides directions for future work.

II. COUPLING IN PRIOR DESIGN OF THE TOOL

A. Design description

Fig. 3 shows the previous design of the tool where the joints of the wrist and yaw axes are mechanically coupled.

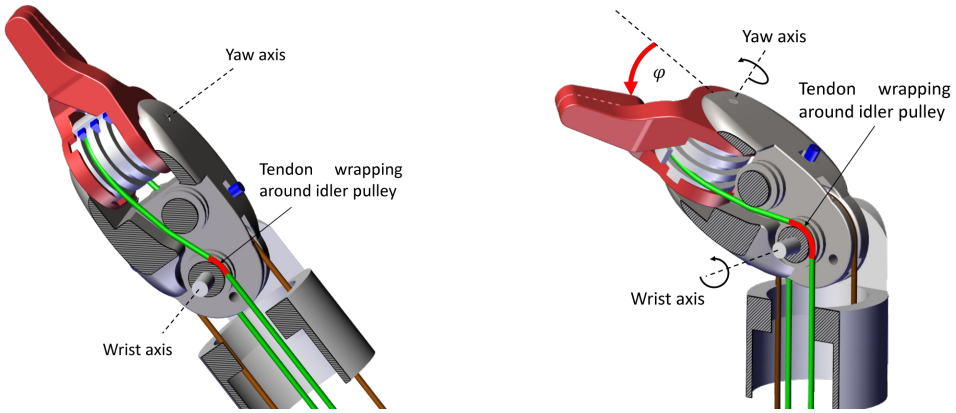

(a) (b)

Fig. 4: The coupling between the joints in the prior design. The wrist actuation forces the graspers to rotate about yaw axis.

The two graspers 5An and 5Bn rotates about the yaw axis with the help of the two pulleys 6An and 6Bn. The rotation of the central pulley 7n drives the two graspers to move linearly in different directions. The linear motion of the graspers causes the rolling of the needle as shown in Fig. 3(d). The mechanism that converts the rotation of the pulley into a linear displacement is illustrated in Fig. 3(c). In this mechanism, the two eccentric cylinders of the central pulley, (7n-1 Fig. 3(c)), rotate eccentrically inside the slots of the graspers. Due to the phase shift of 180° between the two cylinders, one of the graspers moves up and the other moves down. In order to constraint the linear motion of the graspers to be only in their major direction, linear guides (6An-1 Fig. 3(c)) are made on the pulleys 6An and 6Bn.

The actuation of the three pulleys 6An, 6Bn and 7n is made by three pairs of tendons. The tendons are extended from the wrist to the graspers across a set of idler pulleys as shown in Fig. 4. The gripper wrist is actuated by an additional pair of tendons while the tool is driven to rotate about its roll axis by another additional pair.

B. Joint coupling Analysis

Due to the coupling between the wrist and yaw DOFs, when the wrist is actuated, the pulleys of the graspers 6An, 6Bn, and 7n rotate undesirably with an angle φ about the yaw axis, Fig. 4(b). This unsought rotation is compensated by the control algorithm to obtain a pure rotation about the wrist axis. Fig. 4(a) and 4(b) show the routing of the tendons through the idler pulleys before and after the actuation of the wrist. It is shown that when the gripper rotates about the wrist axis, an additional part of the tendon (see the red part in Fig. 4(a) and 4(b)) wraps around the wrist pulley. Consequently, the pulleys 6An, 6Bn, and 7n will rotate with an angle φ to compensate the wrapped part of the tether. Simultaneously, an equivalent part of the tether will unwrap from the wrist pulley on the other side of the gripper. To eliminate the undesired effect of the coupling between the joints, all actuators are driven simultaneously in a coordinated manner by the control algorithm, which is known as software/electronic decoupling. The matrix of eq.

TABLE I: Diameters of the tool pulleys

Parameter	Definition	Value
D_{M1}	Diameter of the roll axis driving pulley	15mm
D_{M2}	Diameter of the wrist axis driving pulley	5mm
D_{M3}	Diameter of grasper-1 driving pulley	5mm
D_{M4}	Diameter of grasper-2 driving pulley	5mm
D_{M5}	Diameter of the sliding motion driving pulley	5mm
D_{P1}	Diameter of roll axis driven pulley	10mm
D_{P2}	Diameter of wrist axis driven pulley	5.5mm
D_{P3}	Diameter of grasper-1 driven pulley	4.5mm
D_{P4}	Diameter of grasper-2 driven pulley	4.5mm
D_{P5}	Diameter of the sliding motion driven pulley	4.5mm
D_{MI}	Diameter of the Idler pulley	3.5mm

(1) is the coupling matrix that describe the relation between the motors rotational angles and the gripper joints angles.

$$\begin{bmatrix} P_1 \\ P_2 \\ P_3 \\ P_4 \\ P_5 \end{bmatrix} = \begin{bmatrix} a_1 & 0 & 0 & 0 & 0 \\ 0 & a_2 & 0 & 0 & 0 \\ 0 & a_3 & a_4 & 0 & 0 \\ 0 & a_5 & 0 & a_6 & 0 \\ 0 & a_7 & a_8 & a_9 & a_{10} \end{bmatrix} \begin{bmatrix} M_1 \\ M_2 \\ M_3 \\ M_4 \\ M_5 \end{bmatrix} \quad (1)$$

where M_i is the rotational angle of the gripper motors that drive the DOFs: roll, wrist, yaw of grasper 1, yaw of grasper 2, and yaw of the central pulley respectively. While, P_i is the rotational angle of the driven pulleys on the gripper side for the DOFs: roll, wrist, yaw of grasper 1, yaw of grasper 2, yaw of the central pulley respectively. The variable a_i is a function of the pulleys' diameters (see table I). In eq. (2), the variables are replaced by their numeric values.

$$a_1 = \frac{D_{M1}}{D_{P1}}, \quad a_2 = \frac{D_{M2}}{D_{P2}}, \quad a_3 = \frac{D_{M2}}{D_{P2}}\frac{D_{MI}}{D_{P3}}, \quad a_4 = \frac{D_{M3}}{D_{P3}},$$
$$a_5 = \frac{D_{M2}}{D_{P2}}\frac{D_{MI}}{D_{P4}}, \quad a_6 = \frac{D_{M4}}{D_{P4}}, \quad a_7 = \frac{D_{M2}}{D_{P2}}\frac{D_{MI}}{D_{P5}},$$
$$a_8 = \frac{1}{2}\frac{D_{M3}}{D_{P3}}, \quad a_9 = \frac{1}{2}\frac{D_{M4}}{D_{P4}}, \quad a_{10} = \frac{D_{M5}}{D_{P5}}$$

$$\begin{bmatrix} P_1 \\ P_2 \\ P_3 \\ P_4 \\ P_5 \end{bmatrix} = \begin{bmatrix} 1.5 & 0 & 0 & 0 & 0 \\ 0 & 0.9 & 0 & 0 & 0 \\ 0 & 0.7 & 1.1 & 0 & 0 \\ 0 & 0.7 & 0 & 1.1 & 0 \\ 0 & 0.7 & 0.55 & 0.55 & 1.1 \end{bmatrix} \begin{bmatrix} M_1 \\ M_2 \\ M_3 \\ M_4 \\ M_5 \end{bmatrix} \quad (2)$$

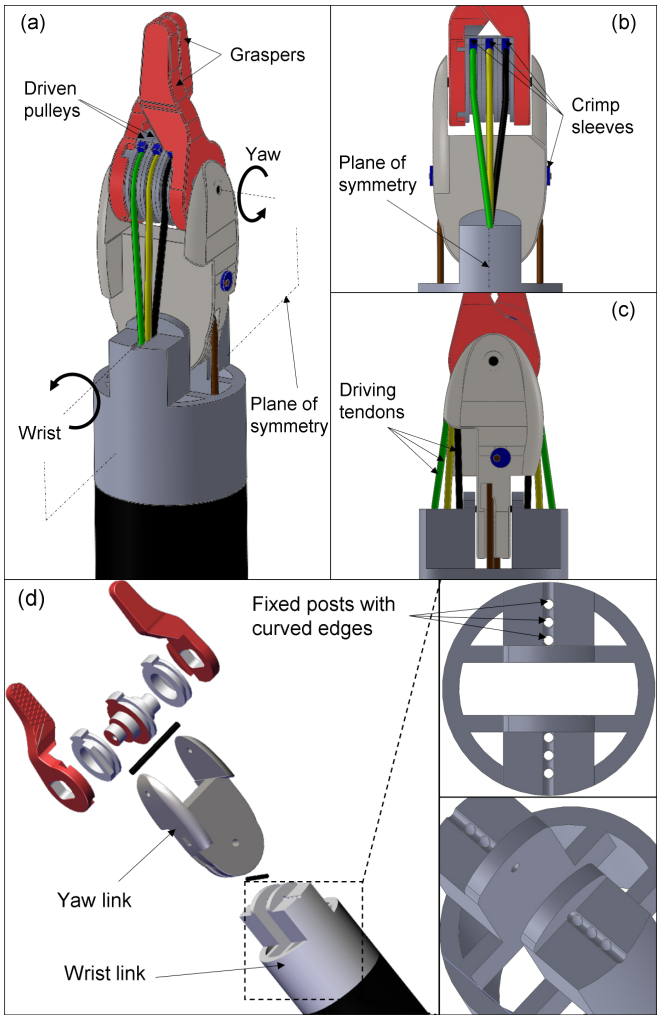

Fig. 5: New tool design with decoupled wrist

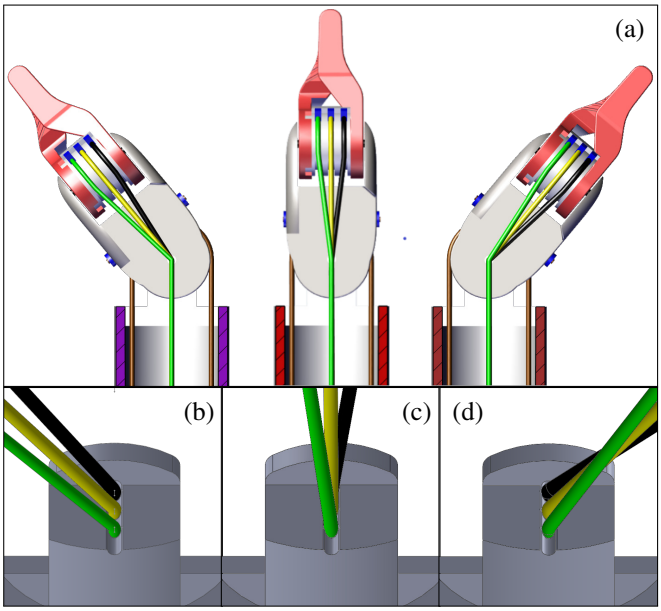

Fig. 6: The gripper rotation about the wrist axis is decoupled from all other joints. The tendons seem to have a sharp bending due to the very small radius of the fixed tubes.

III. NEW DESIGN WITH DECOUPLED WRIST AND ROLLING CAPABILITIES

This section presents the new design of the tool with decoupled wrist. The proposed design has the following features: 1) the tendons are extended through the plane of symmetry of the gripper wrist until reaching the pulleys on yaw axis; 2) the fixed posts, that guide the tendons at the gripper wrist, have curved edges in order to let the tendons move smoothly without being frayed; 3) the design of the fixed posts does not cause the tendons to be significantly stretched to avoid any undesired rotation of the joints; 4) the new design satisfies the constraints of the original design i.e. the outer diameter of the gripper is smaller than the internal diameter of the original trocar used by da Vinci surgical robot.

Fig. 5 shows the proposed design where the tendons, that drive the graspers, are extended through the plane of symmetry of the tool from the wrist link to the driven pulleys on yaw axis. The wrist link has 3 pairs of holes through which the 3 pairs of the driving tendons are routed. A set of crimp sleeves are used to connect the ends of the tendons to the driven pulleys. The design allows all driven pulleys to rotate in the range of $\pm 90°$. The green and black tendons are connected to the two pulleys by which the two graspers can rotate about the yaw axis. The yellow tendon is connected to the central pulley that drive the graspers to make the linear displacement. While the brown tendons, shown in Fig. 5(b) and 5(c), drive the gripper to rotate about the wrist axis. The law of belting is partially followed as two out of the four pairs of tendons i.e. the yellow and brown, have their centrelines aligned with the midlines of the driven pulleys. While the other tendons i.e. the green and black, approach the driven pulleys with small inclination angle that did not show any significant effect during the experiments. To apply the law of belting on all tendons, it requires adding a set of guides and changing the pulleys diameters. This solution is not preferred for two reasons; firstly it complicates the design and the manufacturing process. Secondly, the pulleys diameters of our design are same like those of da Vinci tools which proofed efficiency during the long time use. Fig. 6 shows the rotation of the gripper about the wrist axis with no change in the lengths of the tendons at any rotational angle. Fig. 6(b), 6(c) and 6(d) show the bending of the tendons at the curved edges of the fixed posts.

Equation (3) represents the transmission matrix of the new design with decoupled wrist. The values in the second column show how the gripper joints respond to the rotation of the wrist actuator. Since all values of the second column are zeros, except of the second row that represents the wrist joint, then the wrist motor will only actuate the wrist joint. The transmission matrix is almost diagonal except for the last

row that represents the rotation of the central pulley. The non-diagonal elements show that the rotation of the central pulley is due to the summation of two angles; the first is equivalent to the desired linear displacement of the graspers, and the second is equivalent to the rotation of the two graspers to avoid undesired relative displacement between them.

$$\begin{bmatrix} P_1 \\ P_2 \\ P_3 \\ P_4 \\ P_5 \end{bmatrix} = \begin{bmatrix} 1.5 & 0 & 0 & 0 & 0 \\ 0 & 0.9 & 0 & 0 & 0 \\ 0 & 0 & 1.1 & 0 & 0 \\ 0 & 0 & 0 & 1.1 & 0 \\ 0 & 0 & 0.55 & 0.55 & 1.1 \end{bmatrix} \begin{bmatrix} M_1 \\ M_2 \\ M_3 \\ M_4 \\ M_5 \end{bmatrix} \quad (3)$$

IV. ACTUATION UNIT

Fig. 7 shows the drive box that actuates the new tool. The tendons are routed from the box to the gripper through the tool shaft that has an inner diameter of 7 mm, and outer diameter of 8.5 mm. The drive box has five DC servo motors (MG995), stacked next to each other and coupled with five pulleys/capstans numbered from 1 to 5 as shown in Fig. 7. Every capstan has two grooves hosting a pair of tendons as illustrated in the close-up view of Fig. 7. One tendon extends from the first groove to the corresponding joint, and the other tendon extends from the same joint to the second groove. Capstans 1 and 3 drive the rotation of the two graspers about the yaw axis. Capstans 4 and 5 drive the rotation of the gripper about the wrist and roll axes respectively. Capstan 2 rotates the central pulley about the yaw axis in order to move the two graspers up and down. The tool is mounted on the actuation unit by means of ball-bearing, while a set of idler pulleys are used to route the tendons through the tool shaft to reach the corresponding joints. Fig. 8 gathers all degrees of freedom that can be performed by the gripper. Fig. 8(a) and 8(d) show the rotation of the two graspers about the yaw axis when actuated by capstans 1 and 3. Fig. 8(b) and 8(e) show the linear displacement of the graspers that allows rolling the suture needle. Fig. 8(c) and 8(f) show the sharp bending of the graspers clockwise and counter-clockwise. Fig. 8(g), 8(h) and 8(i) show the rotation of the gripper about the roll and wrist axes when actuated by capstans 5 and 4 respectively.

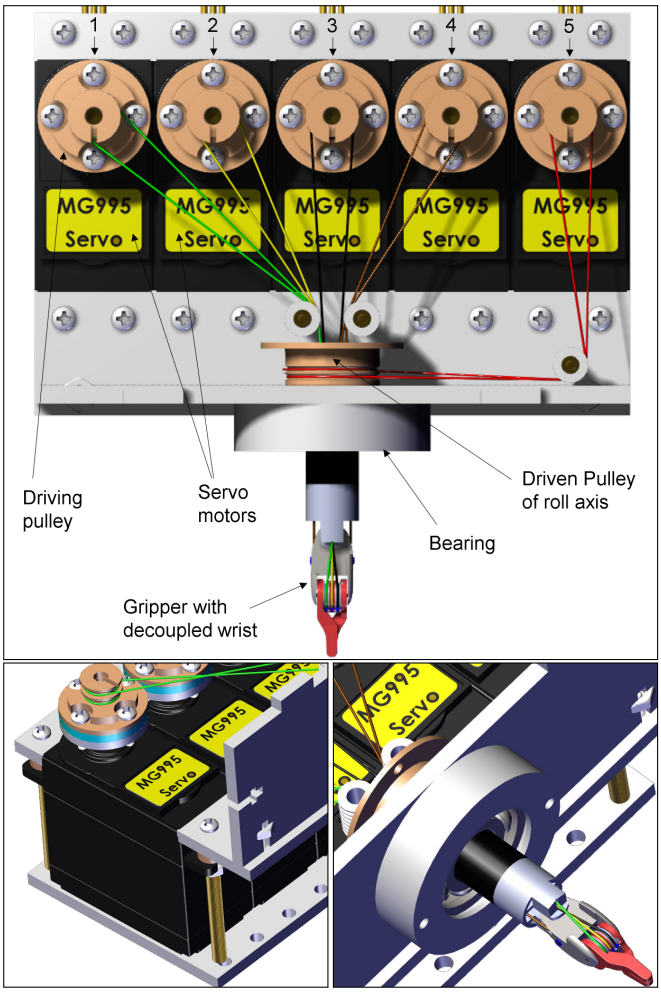

Fig. 7: Drive box with five actuators for the developed tool

V. KINEMATIC MODEL

This section presents the kinematic model of the new tool with decoupled mechanism. Fig. 9 shows the schematic diagram of the tool while the Denavit-Hartenberg frames assigned on the links. The overall structure rotates about the roll axis with an angle θ_1, while the gripper can rotate about the wrist axis with an angle θ_2. The distance from the base frame to frame 1 is l_1; this distance represents the total length of both the tool shaft and wrist link. The distance from frame 1 to frame 2 is l_2; this distance represents the length of the yaw link. The grasping components, that include the two graspers and the three pulleys in between, rotate about the yaw axis with an angle θ_3. Practically, the two graspers always rotate together with the same angle if an object is grasped, so the rotation of both graspers is represented by

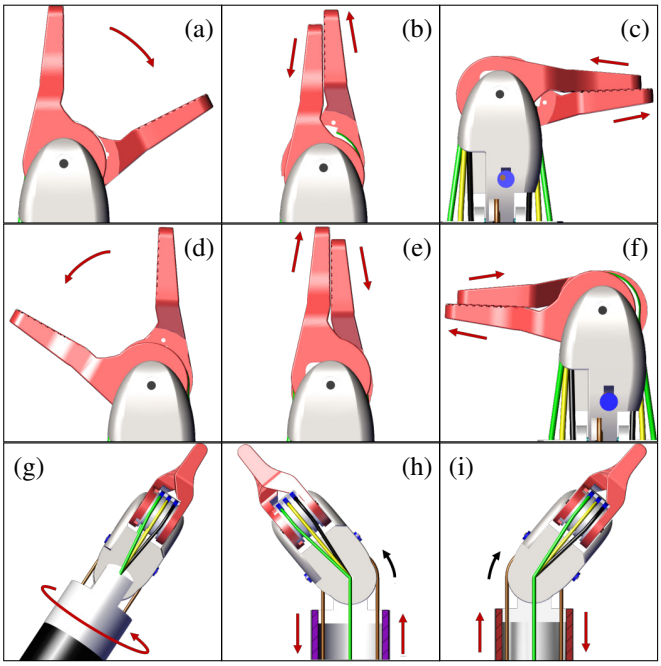

Fig. 8: DOFs of the proposed decoupled tool

TABLE II: D-H parameters of the tool

Link	Joint	a_i	α_i	d_i	θ_i
1	R	0	90	l_1	θ_1
2	R	l_2	90	0	θ_2+90
3	R	l_3	0	0	θ_3

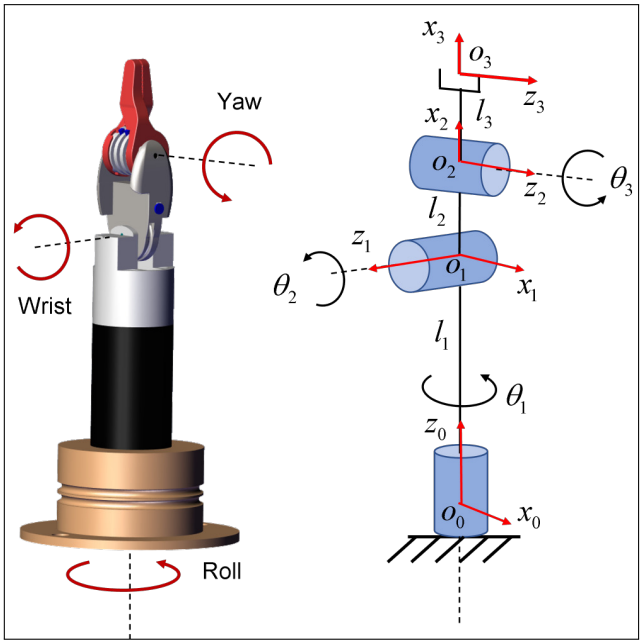

Fig. 9: Tool kinematic diagram with D-H frames

only one angle. Similarly, the rotation of the central pulley does not affect on the position and orientation of the gripper end effector, so it is not represented in the model.

VI. PROTOTYPING AND TESTING

Fig. 10 shows the 3D printed prototype of the new tool with decoupled wrist. The two graspers and their driving pulleys are printed in metal to provide strong grasping force and experience less friction compared with the PLA resin commonly used by 3D printers. Fig. 11 shows the developed actuation unit after mounting the tool and extending the tendons from the motors to the gripper joints. The five motors of the actuation unit are used to drive-by-wire the five degrees

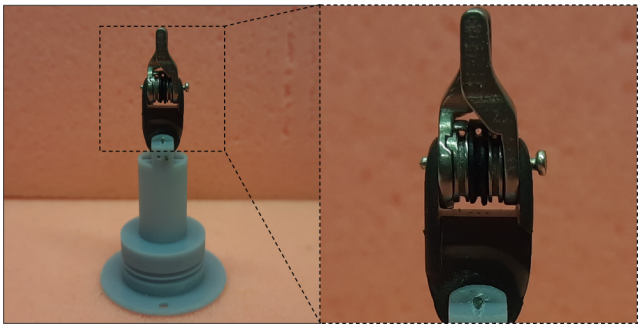

Fig. 10: Tool prototype; the grasping parts are 3D printed in metal to have enough rigidity

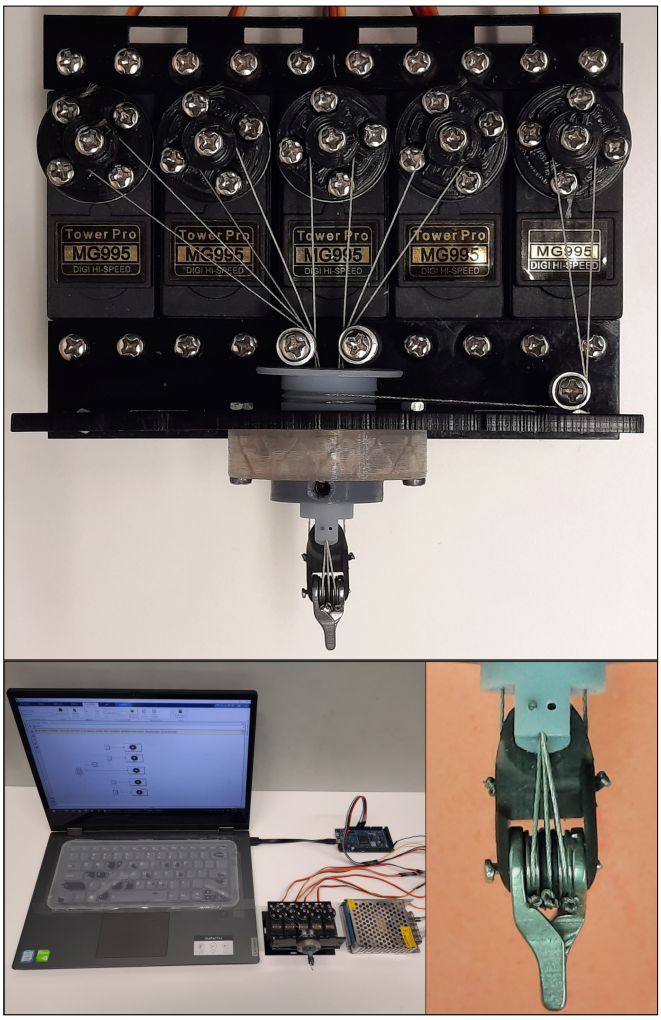

Fig. 11: The experimental setup. The actuation unit drives-by-wire the tool DOFs while the motors are controlled by an Arduino board.

of freedom of the gripper. The close-up view in Fig. 11 shows the crimp sleeves at the ends of the tendons after going through small holes made on the pulleys specifically for this purpose. As shown in the experimental setup, the motors of the driving unit are powered by 5v DC power supply, and controlled by the development kit of Arduino Mega 2560. Matlab/SIMULINK with the Support Package for Arduino is used as a programming environment to communicate with the controller of our setup. The environment allows us to use the kinematic model to generate desired rotational angles and send them as references to the corresponding actuators. In the first experiment, the decoupling between the wrist and yaw axes is tested. In the prior design [28], due to the coupling between the yaw and wrist, the rotation of the gripper about the wrist axis will force the graspers to rotate undesirably about the yaw axis as well, Fig. 4(d). Consequently, the perpendicular distance from the end effector to the axis of rotation (wrist axis in this case) will change due to the bending of the graspers about the yaw axis. However, in the new decoupled design, when the wrist is actuated, the

graspers will not bend. As such, the distance from the end effector to the wrist should be always same at any angle of rotation.

In our experiment, a set of angles ranging from 20° to 160° are sent as references to the motor of the wrist. At the same time, the distance of the end effector with respect to the wrist axis is measured at some selected angles. Fig. 12 shows the rotation of the gripper about the wrist axis while the measured distance is represented by a yellow line. The measuring points are made clear by adding two markers, i.e. green and red. The graph shown in Fig. 12 represents the measured distances in the whole range of the gripper rotation. According to the kinematic model, the distance between the end effector and wrist axis should be always 19.2 mm; represented by the blue line in the graph. The graph shows that the measured distance (the red line) is fluctuating around 18.9 mm with slight variation of 1%. This variation is due to the inaccuracies of the measurement process as the yellow line is extended manually between the measuring points after importing the image into the Matlab workspace. Although this measurement technique is not very accurate, it still reliable enough to make our conclusion as the variation of the readings is random with no specific pattern. On the other hand, the graph shows a slight difference of around 0.3 mm between the estimated distance and the average of the measured distances. This difference is due to the misalignment between the graspers and the wrist link at the beginning of the experiment as the assembly of the gripper is made manually.

In the second experiment, the gripper motion capabilities are demonstrated. Fig. 13 shows a set of different manoeuvrers that could be performed by the gripper. Fig. 13(a), 13(b), and 13(c) show the actuation of the graspers about the yaw axis. Fig. 13(d) and 13(e) show the linear displacement that allows the gripper to roll an object. Fig. 13(f) and 13(g) show the actuation of the gripper about the wrist axis. In addition, the rolling capabilities are tested successfully in presence of a suture needle as shown in Fig. 14.

The decoupling between the wrist and yaw axes could be also verified by conducting a third experiment in which we change the graspers bending and check if the wrist position is affected. Actually, this test was already performed as part of the second experiment when the tool functionalities were under evaluation. The two graspers were commanded to rotate around the yaw, and the wrist was observed not make any undesired motion. Although no measurements were acquired in this test, the attached supplementary video makes it very clear. Moreover, the decoupling is actually inherent in the proposed design, but the experiments were conducted to verify the validity of the whole needle driver after design modifications in terms of workspace, manufacturability and manipulability.

VII. CONCLUSIONS AND FUTURE WORKS

The design and prototyping of a surgical gripper with decoupled wrist and rolling capabilities are presented in this

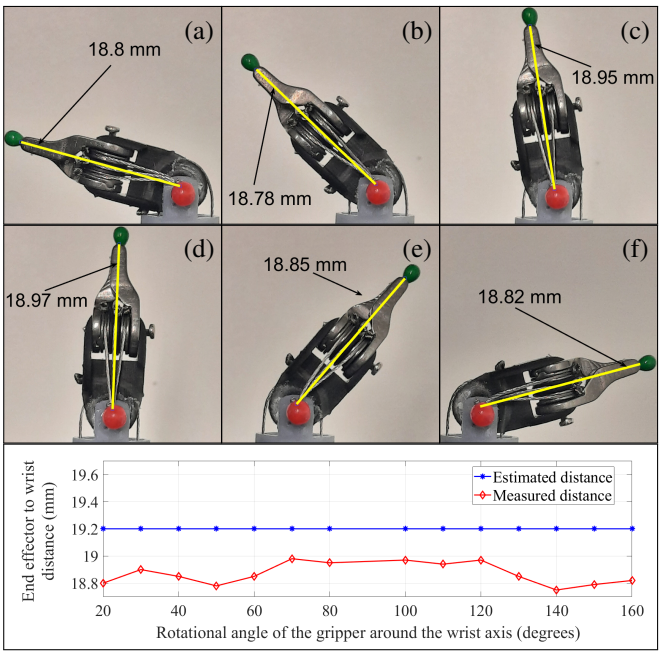

Fig. 12: The results of the first experiment; the gripper is actuated about the wrist while the distance from the end effector to the wrist axis is measured. At any angle of rotation, the distance is almost constant with slight variation of 0.01.

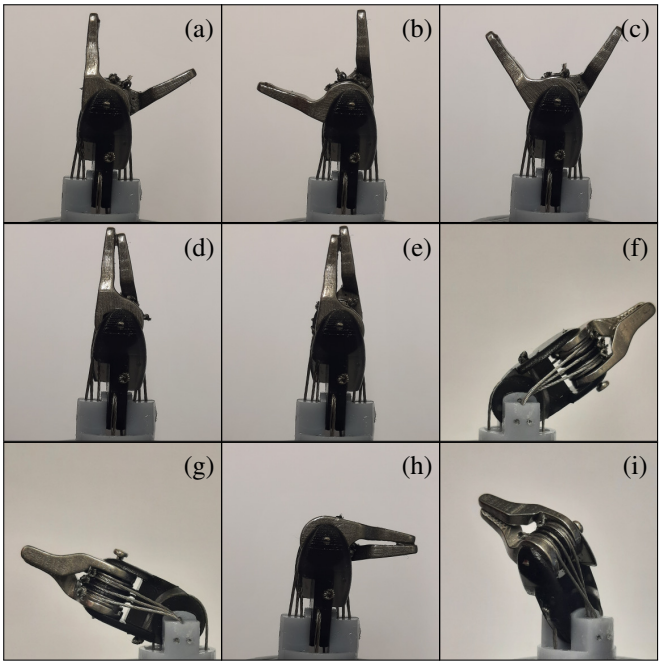

Fig. 13: The results of the second experiment; the motion capabilities of the tool are demonstrated

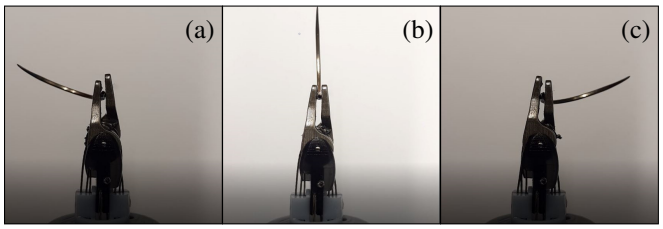

Fig. 14: The rolling capabilities of the gripper is demonstrated in presence of a sutur needle

work. The gripper can be used as a needle driver in robotic-assisted surgeries. The decoupling mechanism is designed based on the approach of routing the tendons through the plane of symmetry of the gripper wrist across fixed posts. An actuation unit with five motors is realized to drive and test the developed prototype. The proposed design is validated with two experiments; in the first experiment the gripper is actuated to rotate about the wrist axis, and at the same time the distance between the end effector and wrist axis is measured. The results validate the proposed decoupling mechanism as the measured distance did not show significant change over the range of rotation. On the other hand, the motion capabilities of the gripper are demonstrated by actuating the different degrees of freedom to have the commonly used configurations. Moreover, the gripper could successfully use its rolling capabilities to change the orientation of a suture needle. The only drawback of the proposed design is the potential reduction in transmission efficiency due to added friction. However, no substantial effect was observed during conducted the experiments. In future work, the gripper should be tested in a real working environment while controlled by a master device.

REFERENCES

[1] G. A. Fontanelli, F. Ficuciello, L. Villani, and B. Siciliano, "Modelling and identification of the da vinci research kit robotic arms," in *2017 IEEE/RSJ International Conference on Intelligent Robots and Systems (IROS)*, 2017, pp. 1464–1469.

[2] R. Moccia, C. Iacono, B. Siciliano, and F. Ficuciello, "Vision-based dynamic virtual fixtures for tools collision avoidance in robotic surgery," *IEEE Robotics and Automation Letters*, vol. 5, no. 2, pp. 1650–1655, 2020.

[3] Intuitive. (2022) Preliminary fourth quarter and full year 2021 results. [Online]. Available: https://isrg.intuitive.com/news-releases/news-release-details/intuitive-announces-preliminary-fourth-quarter-and-full-year-1

[4] J. Marescaux and M. Diana, "Gastrointestinal surgery," in *Robotic Surgery: Applications and Advances*, D. O. Kendoff and A. D. Pearle, Eds. London: Future Medicine LtdUnitec House, 2013, ch. 3, pp. 34–49.

[5] F. Ficuciello, V. A., T. Lisini Baldi, and D. Prattichizzo, "A human gesture mapping method to control a multi-functional hand for robot-assisted laparoscopic surgery: The musha case," *Front. Robot. AI*, vol. 8, 2021.

[6] H. Liu, M. Selvaggio, P. Ferrentino, R. Moccia, S. Pirozzi, U. Bracale, and F. Ficuciello, "The musha hand ii:a multifunctional hand for robot-assisted laparoscopic surgery," *IEEE/ASME Transactions on Mechatronics*, vol. 26, no. 1, pp. 393–404, 2021.

[7] B. Zhao and C. A. Nelson, "Decoupled Cable-Driven Grasper Design Based on Planetary Gear Theory," *Journal of Medical Devices*, vol. 7, no. 2, 06 2013.

[8] C.-H. Kuo, J. S. Dai, and P. Dasgupta, "Kinematic design considerations for minimally invasive surgical robots: an overview," *The International Journal of Medical Robotics and Computer Assisted Surgery*, vol. 8, no. 2, pp. 127–145, 2012.

[9] G. A. Fontanelli, L. R. Buonocore, F. Ficuciello, L. Villani, and B. Siciliano, "An external force sensing system for minimally invasive robotic surgery," *IEEE/ASME Transactions on Mechatronics*, vol. 25, no. 3, pp. 1543–1554, 2020.

[10] A. Petit., F. Ficuciello., G. A. Fontanelli., L. Villani., and B. Siciliano., "Using physical modeling and rgb-d registration for contact force sensing on deformable objects," in *Proceedings of the 14th International Conference on Informatics in Control, Automation and Robotics - Volume 2: ICINCO,*, INSTICC. SciTePress, 2017, pp. 24–33.

[11] B. Zhao and C. A. Nelson, "Estimating Tool–Tissue Forces Using a 3-Degree-of-Freedom Robotic Surgical Tool," *Journal of Mechanisms and Robotics*, vol. 8, no. 5, 05 2016.

[12] K. Grace, "Rigidlylinked articulating wrist with decoupled motion transmission," U.S. Patent 8 292 916B2, Oct. 23, 2012.

[13] K. Nishizawa and K. Kishi, "Development of interference-free wire-driven joint mechanism for surgical manipulator systems," *Journal of Robotics and Mechatronics*, vol. 16, no. 2, pp. 116–121, 2004.

[14] D. S. Kwon, W. H. Shin, and M. H. Hwang, "Surgical robot hand with decoupled wrist structure," International application Patent WO2014/025 204 A1, Feb. 13, 2014.

[15] M. R. Moreyra, "Wrist with decoupled motion transmission," U.S. Patent 2003/0 208 186 A1, Nov. 6, 2003.

[16] K. Tadano and K. Kawashima, "Development of 4-dofs forceps with force sensing using pneumatic servo system," in *Proceedings 2006 IEEE International Conference on Robotics and Automation, 2006. ICRA 2006.*, 2006, pp. 2250–2255.

[17] R. G. Budynas and J. K. Nisbett, *Shigley's Mechanical Engineering Design*. New York: McGraw-Hill, 2011.

[18] D. L. Brock and W. Lee, "Surgical instrument," U.S. Patent 7 744 622 B2, June 29, 2010.

[19] F. Mei, F. Yili, P. Bo, and Z. Xudong, "An improved surgical instrument without coupled motions that can be used in robotic-assisted minimally invasive surgery," *Proceedings of the Institution of Mechanical Engineers, Part H: Journal of Engineering in Medicine*, vol. 226, no. 8, pp. 623–630, 2012.

[20] G. Niu, B. Pan, F. Zhang, H. Feng, and Y. Fu, "Improved surgical instruments without coupled motion used in minimally invasive surgery," *The International Journal of Medical Robotics and Computer Assisted Surgery*, vol. 14, no. 6, p. e1942, 2018.

[21] F. Jelínek, R. Pessers, and P. Breedveld, "DragonFlex Smart Steerable Laparoscopic Instrument," *Journal of Medical Devices*, vol. 8, no. 1, 01 2014.

[22] K. Xu and N. Simaan, "Actuation compensation for flexible surgical snake-like robots with redundant remote actuation," in *Proceedings 2006 IEEE International Conference on Robotics and Automation, 2006. ICRA 2006.*, 2006, pp. 4148–4154.

[23] P. A. E. Francis, "Design and modelling of a miniature instrument for robotic surgery," Master's thesis, University of Toronto, Ontario, Canada, 2017.

[24] *A Compact 2 Degree of Freedom Wrist for Robot-Actuated Surgery and Other Applications*, ser. International Design Engineering Technical Conferences and Computers and Information in Engineering Conference, vol. Volume 5A: 40th Mechanisms and Robotics Conference, 08 2016.

[25] M. Jinno, "Simple noninterference mechanism between the pitch and yaw axes for a wrist mechanism to be employed in robot-assisted laparoscopic surgery," *ROBOMECH Journal*, vol. 6, no. 1, 2019.

[26] K. Chandrasekaran and A. Thondiyath, "Design of a tether-driven minimally invasive robotic surgical tool with decoupled degree-of-freedom wrist," *The International Journal of Medical Robotics and Computer Assisted Surgery*, vol. 16, no. 3, p. e2084, 2020.

[27] A. Spiers, S. Baillie, T. Pipe, and R. Persad, "Experimentally driven design of a palpating gripper with minimally invasive surgery considerations," *Haptics Symposium 2012*, pp. 261–266, 2012.

[28] G. A. Fontanelli, M. Selvaggio, L. R. Buonocore, F. Ficuciello, L. Villani, and B. Siciliano, "A new laparoscopic tool with in-hand rolling capabilities for needle reorientation," *IEEE ROBOTICS AND AUTOMATION LETTERS*, vol. 3, no. 3, pp. 2354–2361, 2018.